Polygonal Wear of Automobile Tire*

Atsuo SUEOKA**, Takahiro RYU**,
Takahiro KONDOU***, Minoru TOGASHI****
and Toshiro FUJIMOTO*****

This study investigates, experimentally and analytically, the polygonal wear of truck/bus and car tire and elucidates the generation mechanism of polygonal wear caused by the first natural vibration mode of the tire in the vertical direction. In the analysis, the phenomenon is modeled as a time delay system accompanied by wear in which the amount of wear of the tire is fed back as forced displacement in the vertical direction after the time period of tire rotation. The progress of the polygonal wear of the tire is very slow and is caused by unstable vibration in the steady-state wear process generated in the limited regions where the products of polygonal numbers and the rotational speed of the tire are less than the natural frequencies of the tire system. The tire is deformed almost to the shape of a regular polygonal when polygonal wear occurs. Good agreement between experimental and analytical results concerning the occurrence of polygonal wear of the tire was confirmed.

Key Words: Stability, Vibration of Rotating Body, Contact Vibration, Pattern Formation, Modeling, Wear, Automobile Tire, Polygonal Wear, Self-Excited Wear

1. Introduction

In the field of mechanical engineering, a number of contact rotating systems are used. While operating of the contact rotating systems, periodic polygonal deformation patterns are formed on the peripheral surface of a roll which is a rotating body due to viscoelastic deformation, plastic deformation and cutting, grinding and wear, and hence they eventually lead to a situation where the systems become no longer operative[1]. In this report, we call such phenomena pattern formations.

There exists a system consisting of road and automobile tires as a typical example of the contact rotating system close to our daily environments. Pattern formation phenomena generated in this system are called abnormal wears in which many wear patterns of heel and toe wear, step down wear, taper wear, center wear, polygonal wear and so on are well known[2),(3]. These wears are generated usually in combination with the inner causes such as tire structure, tire shape, and tread pattern, and with the external causes such as structure of vehicle, wheel alignments (parallelism between right and left wheel tires, for example, toe-in and camber angle; see Fig. 3), maintenance condition, position of installation, speed, load, air pressure, operation of car, road surface condition, configuration of ground and temperature.

In recent years, as the expressways are spread, the driving at high and constant speed for a long time may be in usual way. Following this, the self-excited polygonal wear phenomena are often generated in automobile tires. In Fig. 1(a), an example of the polygonal wear of a truck tire is shown. This is the

* Received 28th February, 1997. Japanese original: Trans. Jpn. Soc. Mech. Eng., Vol. 62, No. 600, C (1996), pp. 3145-3152 (Received 11th January, 1996)
** Department of Mechanical Engineering, Faculty of Engineering, Kyushu University 36, 6-10-1 Hakozaki, Higashi-ku, Fukuoka 812-81, Japan
*** Faculty of Engineering, Fukuoka Institute of Technology, 3-30-1 Wajiro-higashi, Higashi-ku, Fukuoka 811-02, Japan
**** Bridgestone Corporation, 3-1-1 Ogawahigashi-cho, Kodaira 187, Japan
***** Department of Mechanical Engineering, Ube College of Technology, Tokiwadai, Ube 755, Japan

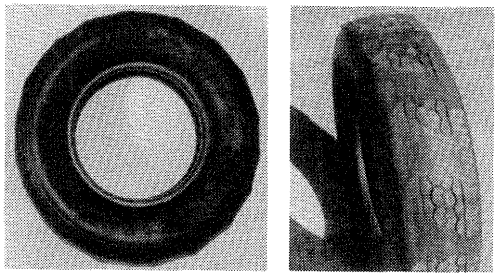

(a) Self-excited polygonal wear

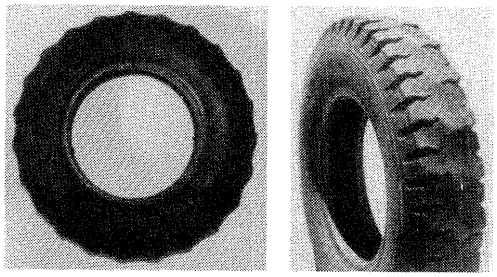

(b) Self-excited polygonal wear including forced excitation

Fig. 1 Examples of polygonal wear

almost regular polygonal wear with polygonal number of 18 in the circumferential direction independent of tread pattern of tire, and the wear pattern seems to be slightly oblique to the axial direction of tire. Figure 1 (b) shows the regular polygonal wear with polygonal number of 23 generated in lug type truck tire in which the wear is generated on every other tread pattern. This kind of wear is easily generated on the tread pattern of tire with large lateral grooves, and this may be an example of the pattern formation including both the self-excited factor and the forced or the parametric factor arising from lug pattern.

In this report, the authors treat experimentally and analytically the self-excited polygonal wear phenomenon which is not directly dependent of the tread pattern of tire and has a certain spatial periodicity in the circumferential direction. And they make clear the generation mechanism of the polygonal wear only phenomenon of which has been well known so far.

2. Features of Polygonal Wear of Tire

First, the particular features of polygonal wear of tire[(1)-(5)] which is generated when passenger cars, trucks and buses are ordinarily traveling on usual roads or expressways are described.

(1) The polygonal wear is generated in not driver wheel tire but follower wheel tire. Especially, we can see many generation examples of the polygonal wear in the rear wheel tires of the FF vehicles.

(2) The polygonal wear is easily generated when the toe-in of the wheel alignments is too large.

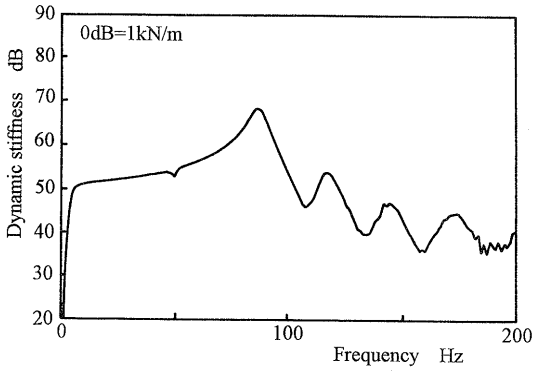

Fig. 2 Dynamic stiffness of a car tire

(3) The polygonal wear is caused by the vibration of the tire itself, and one of its natural frequencies is related directly to the polygonal number of the polygonal wear of tire, that is, the relationship of (natural frequency of tire) $\approx$ (polygonal number of tire) $\times$ (rotational speed of tire) is observed.

(4) The resulting polygonal number of the passenger car tire is different from that of truck/bus tire, but it is wholly equal to 10 to 20.

(5) The polygonal wear grows occasionally from the outside of the shoulder part to the axial direction of tire obliquely (called the diagonal wear). Then, the polygonal wears of tires on the left and right hand sides are in a reflected image such as letter V when inspected from the back. The oblique angle to the axial direction is not corresponding to the slip angle of tire due to the toe-in [see Fig. 3(b)].

(6) The polygonal wear is generated in the order of the distance covered of 25 000 to 40 000 km.

(7) The generation rate of polygonal wear for the tire of the vehicles traveling on the expressway is remarkably high.

(8) The generation rate depends on surface condition of road, temperature, materials of tire and so on. Polygonal wear is easily generated on asphalt road, at high temperature (in summer), and by using the tire with low inner pressure.

(9) Since the polygonal wear is a phenomenon having the frequency higher than 60 Hz, the drivers feel it as unpleasant noise rather than intolerable vibrations.

3. Experimental Results

Figure 2 shows the dynamic stiffness F/X obtained from measuring the axial force F in the vertical direction of a non-rotating tire for the case that a radial tire for passenger car with air pressure 196 kPa is pressed to a shaking table at the load 3.96 kN, and the random forced displacement X in the vertical direction is given. In Fig. 2, we can see the

Table 1 Experimental results of polygonal wear

Tire	Natural frequency f_n (Hz)	Polygonal number for traveling speeds		
		45(km/h)	60(km/h)	70(km/h)
A	73.5	18 (18.84)	14 (14.13)	12 (12.11)
B	69.8	—	13 (13.42)	—

resonance points of the first to the fourth orders in the vertical direction of the tire. The first vibration mode corresponds to the one in which the tread vibrates in the vertical direction, and so this mode generates the large force in the vertical direction on the rotating shaft. The modes higher than the second mode correspond to the elastic vibration ones of tire. The first natural frequency f_n in the vertical direction of a rotating tire is about 70 to 80 Hz for both truck/bus and passenger car[6].

In the followings, we show the experimental results of the polygonal wear caused by the first vibration mode of a truck tire in the vertical direction. The experiment was performed on the indoor large-scaled wear tester by using radial tires for truck and bus. In the experiment, the growth process of the polygonal wear was observed at the constant traveling speed and at a constant press load between tire and drum, setting suitable values of toe-in and camber angle. We used radial tires A and B makers of which are not same. Their effective radius, air pressure and tire loading are 510 mm, 710 kPa and about 23.8 kN commonly, respectively. The rotating shaft of tire is rigidly fixed, and so there exist no objects having the vibration characteristics except tire in the experimental apparatus.

The experimental results are indicated in Table 1 where the relationships between the traveling speeds (45, 60, 70 km/h) and the polygonal numbers of the polygonal wear are shown for tires A and B. The figures indicated in the round bracket are the values calculated from the relationship of (polygonal number of polygonal wear of tire) = (the first natural frequency of tire in the vertical direction f_n) / (rotational speed of tire). Notation "—" shows that the corresponding experiment was not performed. The polygonal number is almost integer in the experiment, but accurately the pattern gets out of position to some degree from regular polygon. We find that some polygonal numbers obtained from the experiment are nearly coincident with the values calculated from the relationship described above, but the others are different from the figures indicated in the bracket. In order to explain the experimental results, the generation mechanism of the polygonal wear is analyzed based on a comparatively simple analytical model in the next chapter.

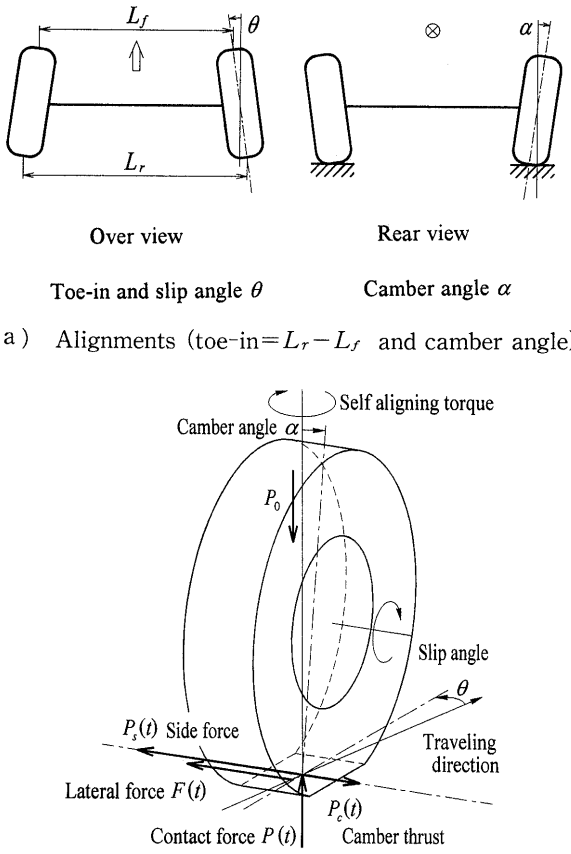

(a) Alignments (toe-in $= L_r - L_f$ and camber angle)

(b) Forces acting on contact surface

Fig. 3 Alignments and forces acting on contact surface

4. Theoretical Analysis

In Fig. 3, the toe-in (or equivalently slip angle) and the camber angle which are both wheel alignments of tire, the forces acting on tire through the contact section between road surface and tire, and their positive directions are shown. The ordinary toe-in (the corresponding slip angle) and the ordinary camber angle of truck/bus radial tire is set to 0 to 6 mm (0 to 0.17°) and 0 to 1.5°, respectively, where the slip angle is equal to 180° × toe-in/(4π × effective radius of tire). The ordinary toe-in and the ordinary camber angle of passenger car radial tire is set to −3 to 5 mm (−0.15 to 0.25°) and 0 to 1°, respectively.

4.1 Analytical model

It was made clear from the experimental results mentioned in chapter 3 that the first natural vibration mode of tire in the vertical direction took part in the polygonal wear. Thus, in this section, the generation mechanism of the pattern formation phenomenon caused by the first natural vibration mode of tire itself in the vertical direction is analyzed based on the simple analytical model as shown in Fig. 4.

For analysis, the following assumptions are made

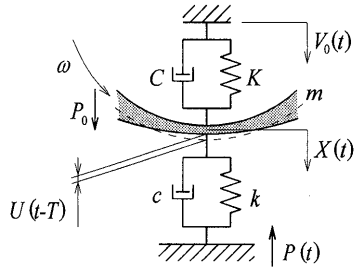

Fig. 4 Analytical model for the fundamental experiment

(see Fig. 4) :

(1) The system treated here is modeled as a single-degree-of-freedom system in which the tread part of tire vibrates in only the vertical direction. The mass of the tread part corresponding to the first natural vibration mode in the vertical direction is m, the contact stiffness and damping coefficient between tire and road surface are k and c, and the spring constant and damping coefficient of side wall are K and C.

(2) Let the initial equilibrium point of the tread part subjected to an initial compression stress be the origin, and let the displacement of the tread part from the initial equilibrium point be $X(t)$.

(3) The instantaneous wear quantity of the tread part in the contact section between tire and road surface depends on only the absolute value of lateral force acting between them. Now, let the total wear quantity of the tread part in the contact section at an instant be $U(t)$. This total wear quantity is fed back to the contact section as a forced displacement $U(t-T)$ in one revolution period of tire (after a time period of tire rotation T). Hence, the analytical modeling treated here yields the system with time lag accompanied by wear.

(4) When the constant compression stress act, and the mass of tread part is not vibrating, the total wear quantity $U(t)$ may be increased at a constant rate, that is, the uniform wear in the circumferential direction of tire can be generated. We call such wear the steady-state wear here. In this investigation, the stability of the steady-state wear is analyzed, regarding the polygonal wear as unstable phenomenon of the steady-state wear caused by the effect of time lag in (3) mentioned above.

(5) In the growth process of the steady-state wear, the foundation of upper part supporting the spring K as shown in Fig. 4 need obviously to move at a constant velocity in the lower direction. Let the constant velocity of this displacement be $V_0(t)$ (see section 4.8). In this analytical model, it is assumed that the displacement at the constant velocity $V_0(t)$ in the lower direction is always given to the foundation of the upper part.

4.2 Contact force $P(t)$ in the vertical direction between tire and road surface

The contact force is transmitted through the spring constant k and damping coefficient c as shown in Fig. 4. From Fig. 4, the contact force $P(t)$ is represented as

$$P(t)=P_0+c\dot{W}_2(t)+kW_2(t) \quad (1)$$

where P_0 is the initial compression force including the gravity force of tire, and

$$W_2(t)=X(t)-U(t-T) \quad (2)$$

In the contact force $P(t)$ expressed as Eq. (1), the effect of time lag is taken into account that some tread part subjected to wear when passing through the rolling contact section at an instant re-enters to the contact section after a time period of tire rotation. Now, initial compression force P_0 is much larger than the fluctuating contact force $c\dot{W}_2(t)+kW_2(t)$, and thus the contact force $P(t)$ is assumed to be always positive.

4.3 Side force $P_s(t)$

For the small slip angle θ, the side force is proportional to the slip angle and the contact force in the vertical direction from the measured results of the various tires, that is,

$$P_s(t)=a_s\cdot P(t)\cdot\theta \quad (3)$$

where a_s is a linear constant. Moreover, since we treat the case where the slip angle is small, the cornering force is nearly equal to the side force.

4.4 Camber thrust $P_c(t)$

For the small camber angle α, the camber thrust is proportional to the camber angle and the contact force in the vertical direction from the measured results of the various tires, that is,

$$P_c(t)=a_c\cdot P(t)\cdot\alpha \quad (4)$$

where a_c is a linear constant. Force $P_c(t)$ is considerably small compared with $P_s(t)$.

4.5 Lateral force $F(t)$ acting on tire

In general, the side force and the camber thrust act in the opposite direction to each other in the case that the slip and the camber angles are both positive (see Fig. 3). Therefore, the lateral force $F(t)$ is approximated as

$$F(t)=P_s(t)-P_c(t)=(a_s\theta-a_c\alpha)P(t) \quad (5)$$

4.6 Wear quantity of tire

The polygonal wear of tire is markedly generated in not the driver wheel tire but the follower wheel one. Taking this experiential fact mentioned above into account, it is rational to regard the main cause of wear on the tire tread part as not the slip in the longitudinal direction (in the direction of progress) but the one in the transverse (axial) direction generated in the rolling contact section between tire and road surface. Moreover, the slip in the transverse direction is in general generated not over the whole rolling

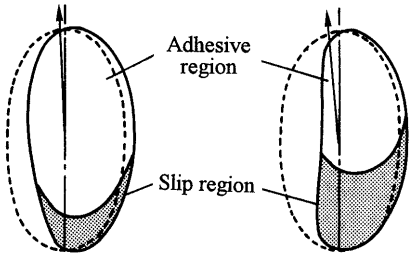

(a) Small slip angle (b) Large slip angle

Fig. 5 Slip and adhesive regions on contact surface

contact section but on a part of the rolling contact section even if the lateral force is markedly large. In reference (5), the wearing part in the contact section was experimentally specified under the condition that the slip or the wear occurs in the regions in which the stress due to friction $\mu\sigma_z$ is smaller than the lateral stress σ_t, where μ is coefficient of friction between tire and road surface in the rolling contact section, and σ_z is normal stress. In general, the adhesive and the slip regions are distributed in the front and the rear parts of the rolling contact section, respectively as shown in Fig. 5 independent of the amplitude of slip angle. In the slip region which spreads over this rear part, the wear due to slip in the transverse direction is generated, and it may lead to the polygonal wear of tire.

Now, in order to explain the generation mechanism of the polygonal wear of tire by using a very simple model, the contact surface between tire and road surface is approximately regarded as a concentrated point (or a remarkably narrow area) on the outer circumference of tire, and we make the point of contact correspond to the slip region mentioned above. Namely, the slip in the transverse direction is necessarily generated at the point of contact between tire and road surface due to wheel alignments such as toe-in. This is the wear model treated here. Then, the instantaneous wear quantity $W(t)$ may be also increased as the contact force and the lateral force become large. Hence, it is assumed that the instantaneous wear quantity $W(t)$ is proportional to the absolute value of $F(t)$ to the n-th power, that is,

$$W(t)=\nu|F(t)|^n=\nu\beta^n\{P(t)\}^n \qquad (6)$$

where $W(t)$ has dimension of length, $\beta=|a_s\theta-a_c\alpha|$, and n is a constant. In addition, ν is a constant which varies with the kinds of tire, temperature, traveling speed and so on, and the reciprocal of ν means so-called the wear resistance.

By the way, the following basic expressions for the instantaneous wear quantity of tire have been reported among the investigations[2),3),7)] so far.

(1) The case that the instantaneous wear quantity is proportional to lateral force: the case of $n=1$ in Eq. (6)

(2) Wear theory according to Schallamach: The present theory mentions that the instantaneous wear quantity which develops into the polygonal wear is increased as the lateral force acting on the contact surface and the slip generated on the contact surface becomes large. Applying this theory to the follower wheel tire, the instantaneous wear quantity is expressed as

$$W(t)=\gamma\rho S|F(t)|=\gamma\rho\{F(t)\}^2/G \qquad (7)$$

where γ is wear rate of tread rubber, ρ is repulsion elasticity of tire, $S=|F(t)|/G$ is rate of slip in the transverse direction in the contact surface of tire, G is lateral stiffness of tire. The constants γ and ρ are decided from the structure and materials of tire. From the above equation, the instantaneous wear quantity according to Schallamach corresponds to the case of $n=2$ in Eq. (6).

On the other hand, the total wear quantity of tire $U(t)$ at the contact point at an instant is expressed as the sum of the total wear quantity $U(t-T)$ before one revolution at that point and the current instantaneous wear quantity $W(t)$, that is, by the following recurrent form:

$$\begin{aligned}U(t)&=U(t-T)+W(t)\\&=U(t-T)+\nu\beta^n\{P(t)\}^n\end{aligned} \qquad (8)$$

4.7 Equation of motion of tire tread

Based on the discussion up to section 4.6, the equation of motion of tire tread in which the initial equilibrium point is set to the origin is given as

$$m\ddot{X}(t)+C\dot{W}_1(t)+KW_1(t)+c\dot{W}_2(t)+kW_2(t)=0 \qquad (9)$$

where $W_1(t)=X(t)-V_0(t)$.

4.8 Steady-state wear solution and its stability

The steady-state wear solution mentioned in section 4.1 corresponds to the one obtained by putting $P(t)=P_0$ in Eq. (8) (hence, $W_2(t)=0$ and $\dot{W}_2(t)=0$ from Eqs. (1) and (2)) and $\ddot{X}(t)=0$, $W_1(t)=0$, $\dot{W}_1(t)=0$ in Eq. (9). Such particular solution is called steady-state wear solution here, and is represented by the variables with subscript 0. The steady-state wear solution is simply calculated as

$$\left.\begin{aligned}U_0(t)&=\nu\beta^nP_0^n(t+T)/T\\X_0(t)&=V_0(t)=U_0(t-T)=\nu\beta^nP_0^nt/T\end{aligned}\right\} \qquad (10)$$

The stability of the steady-state wear solution is determined by investigating the dynamic behavior of the infinitesimal variations. Here, the variation of every variable is expressed by using the small letter corresponding to the variable of capital letter as

$$X(t)=X_0(t)+x(t),\quad U(t)=U_0(t)+u(t) \qquad (11)$$

Substituting Eq. (11) into Eqs. (8) and (9) yields the following equation with respect to the variations:

$$\left.\begin{aligned} &m\ddot{x}(t)+C\dot{x}(t)+Kx(t)+c\{\dot{x}(t)-\dot{u}(t-T)\}\\ &\quad+k\{x(t)-u(t-T)\}=0\\ &u(t)=u(t-T)+\nu\beta^n P_0^{n-1}n[c\{\dot{x}(t)-\dot{u}(t-T)\}\\ &\quad+k\{x(t)-u(t-T)\}]\end{aligned}\right\} \tag{12}$$

In order to make the revolution period of tire be 2π, following variable transformation is applied to Eq. (12):

$$\tau=\omega t,\ \omega=2\pi/T \tag{13}$$

After this transformation, Laplace transformation is applied to Eq. (12) with all the initial values equating to be zero. Then, we obtain

$$\left.\begin{aligned} &\{m\omega^2s^2+(c+C)\omega s+k+K\}\tilde{X}(s)\\ &\quad-(c\omega s+k)e^{-2\pi s}\tilde{U}(s)=0\\ &[\{1-\nu\beta^n P_0^{n-1}n(c\omega s+k)\}e^{-2\pi s}-1]\tilde{U}(s)\\ &\quad+\nu\beta^n P_0^{n-1}n(c\omega s+k)\tilde{X}(s)=0\end{aligned}\right\} \tag{14}$$

where $\tilde{X}(s)$ and $\tilde{U}(s)$ are image functions after Laplace transformation of $x(t)$ and $u(t)$, respectively, and s is a variable for Laplace transformation.

From Eq. (14), the characteristic equation becomes

$$A(s)B(s)+C(s)=0 \tag{15}$$

where

$$A(s)=m\omega^2s^2+(c+C)\omega s+k+K$$
$$B(s)=\{1-\nu\beta^n P_0^{n-1}n(c\omega s+k)\}e^{-2\pi s}-1$$
$$C(s)=\nu\beta^n P_0^{n-1}n(c\omega s+k)^2e^{-2\pi s}$$

Influenced by the time delay elements, countable infinite number of characteristic roots s exist which satisfy Eq. (15). If at least one of these characteristic roots has positive real part (called unstable characteristic root), the steady-state wear solution becomes unstable, and the polygonal pattern is formed on the tire tread with the growth of variations. The imaginary part of the unstable characteristic roots means the polygonal number of the polygonal wear. The Newton-Raphson method is applied to the characteristic equation. There are a finite number of unstable characteristic roots with positive real parts[8].

The polygonal wear phenomenon generated in an actually traveling automobile is treated as coupled vibration among tire tread described above, unsprung and sprung masses in the vertical direction. The analytical model and the numerical computational results are indicated in Appendix.

5. Numerical Computational Results and Discussions

Table 2 shows the values of the constants a_s and a_c for radial tires of truck/bus and passenger car computed from the measured data of the side force and the camber thrust. Moreover, in Table 3 are shown the parameter values corresponding to radial tire A for truck/bus used in the experiment of the polygonal wear. In the numerical computation of this report, we used $\theta=0.5°$, $\alpha=1°$ and $r=510$ mm.

Figure 6(a) shows the relationship between N which is imaginary part of the characteristic root $s(=\sigma+\sqrt{-1}N)$ and rotational frequency $f=\omega/2\pi$ of tire for the case of $n=1$ and $\nu=2.90\times10^{-14}$ m/N. The imaginary part N means the polygonal number of tire. Thick solid lines show unstable regions ($\sigma>0$), that is, the regions in which the polygonal wear is generated. Dotted lines show stable regions ($\sigma\leq0$). Curve Ω_1 shown in Fig. 6 indicates the ratio (f_n/f) of the first natural frequency of tire in the vertical direction to rotational frequency of tire and it is also corresponding to the stable solution. Figure 6(b) shows the distribution of real part σ of the characteristic root in the unstable region corresponding to $N=10$ of Fig. 6(a). From the figure, the computational results are summarized as follows:

(1) The polygonal number of tire when the polygonal wear is generated is an integer, and the smaller is the polygonal number, the higher is the

Table 2 Values of coefficients

Tire	a_s (1/deg)	a_c (1/deg)
Truck and bus Air pressure (784kPa)	0.097	0.0012
Car Air pressure (196kPa)	0.22	0.014

Table 3 Parameters of truck/bus tire

m (kg)	k (MN/m)	c (Ns/m)	K (MN/m)	C (Ns/m)
23.0	1.22	343	3.68	520

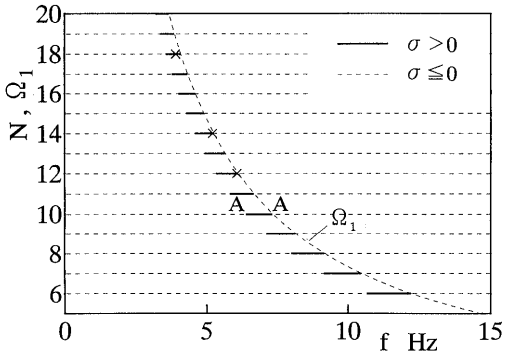

(a) Relationship between f and N

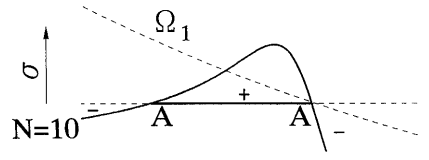

(b) Degree of instability σ in an unstable region

Fig. 6 Unstable regions of polygonal wear

rotational frequency of tire at which the polygonal wear occurs and the wider become the unstable regions. And there are unstable regions on the left hand side of curve Ω_1, that is, the solutions become unstable in the limited regions satisfying the relation of (rotational frequency of tire) $\leq$ (the first natural frequency of tire in the vertical direction) / (polygonal number of polygonal wear). On the other hand, we can not see the unstable regions on the right hand side of curve Ω_1. The case in which the polygonal number N is integer means that the pattern formation arising from the polygonal wear phenomenon is fixed on the tire and grows.

(2) The values of real parts of the unstable characteristic roots are wholly very small. This means that the polygonal wear grows very very slowly. Here, we call the real part of the unstable characteristic root the degree of instability. From the distribution of the degree of instability, it has a peak near the boundary on the right hand side of each unstable region. Near the peak, the polygonal wear is easily generated and grows fast. The maximum values of σ in unstable regions are at most in the order of 10^{-9}. This tendency holds for all polygonal numbers.

(3) Since some unstable regions overlap another unstable one at a certain rotational frequency of tire, the polygonal wears with the different polygonal numbers can be generated simultaneously from the computational results. Though the linear stability theory can not decide which polygonal wear is generated, the polygonal wear whose unstable characteristic roots have larger real part will eventually prevail.

From the numerical computations using various parameters, it was made clear that the width of the unstable regions did not change very much even if the value of ν was widely changed. On the other hand, changing the value of ν gives the influence upon the degree of instability in the unstable regions, that is, upon the values of real parts σ of the unstable characteristic roots. As the value of ν is decreased, the degree of instability becomes low. From this fact, the width of the generation regions of the polygonal wear is not dependent of the constant n very much appearing in Eq. (8) representing the total wear quantity, because the effect of the constant n appears only in the coefficient $\nu\beta^n P_0^{n-1} n$ in the linear analysis using Eq. (15), and changing n is equivalent to changing ν included in coefficient $\nu\beta$ for $n=1$.

On the other hand, the effect of damping coefficient C gives a remarkable influence upon the width of the unstable regions rather than the degree of instability contrary to the effect of ν. Namely, as the damping coefficient C is increased, the unstable regions are become narrow.

Next, the experimental results mentioned above and the result of Fig. 6 are compared. The corresponding experimental points of the polygonal wear for tire A are plotted by symbol $\times$ as shown in Fig. 6. The polygonal wear phenomena generated experimentally are all in the unstable regions in Fig. 6. In the case that the generation regions of the polygonal wear with different polygonal numbers overlap at some traveling speed, the polygonal wear with relatively larger degree of instability which is positioned in the vicinity of the boundary on the right hand side of the unstable region may be dominantly generated as mentioned above. In such a way, a very good correspondence between the experimental results of the polygonal wear using radial tire for truck and the analytical ones using a simple analytical model was confirmed, and thus, the generation mechanism of the polygonal wear was made clear.

As described above, it was made clear from the basic experiment and analysis that the main generation cause of the polygonal wear is the unstable vibration caused by the first natural vibration mode of tire in the vertical direction. Next, the numerical computational results of the polygonal wear of tire for the case that the actual vehicle is traveling on the road will be presented.

Figures 7 and 8 show the unstable regions in

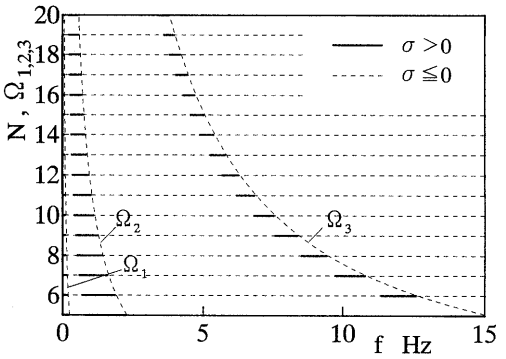

Fig. 7 Polygonal wear regions of a truck tire

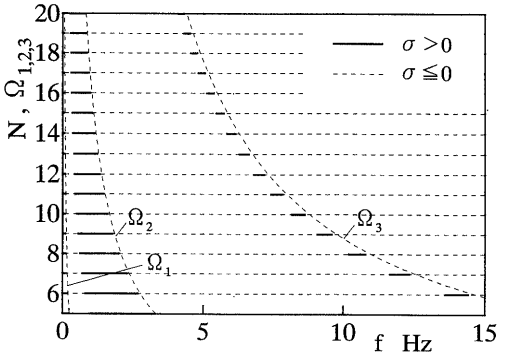

Fig. 8 Polygonal wear regions of a car tire

Table 4 Parameters for numerical computation

Vehicle	r (mm)	m_1 (kg)	m_2 (kg)	m_3 (kg)	k_1 (MN/m)
Truck	510	23.0	186	2250	1.22
Car	300	4.6	20.0	300	0.299
Vehicle	k_2 (MN/m)	k_3 (kN/m)	c_1 (Ns/m)	c_2 (Ns/m)	c_3 (Ns/m)
Truck	3.68	118	343	520	2430
Car	0.941	19.6	98	147	490

which the polygonal wear is generated using the parameters indicated in Tables 2 and 4, and $n=1$. Figures 7 and 8 are the results of truck tire and passenger car tire for the case of $\nu=2.90\times10^{-14}$ and 1.09×10^{-13} m/N, respectively. Not only the polygonal wear caused by the first vibration mode of tire in the vertical direction which corresponds to the third mode (Ω_3) of the system consisting of tread, sprung and unsprung masses but also the polygonal wear caused by the first and the second modes (Ω_1 and Ω_2) in which the sprung and the unsprung masses mainly vibrate, respectively, are generated. However, as the natural frequencies of the first to third modes are distinct from each other, the tendency of the polygonal wear caused by the first mode of tire in the vertical direction is almost the same as that of Fig. 6.

By the way, Figs. 6, 7 and 8 show the generation regions of polygonal wear for the case of constant traveling speed. Actually, the cars repeat start and stop, therefore, the constant traveling speed is not held continuously, and the condition of road surface changes also. Thus, if the rotational frequency of tire remains in an unstable region with some polygonal number in spite of the fluctuation, the polygonal wear with the polygonal number grows gradually at least. If the rotational frequency of tire goes out from the unstable region, the polygonal wear with the polygonal number disappears or the one with another different polygonal number may start growing.

As mentioned above, the generation mechanism of the polygonal wear is made clear experimentally and theoretically. However, it is difficult to explain the generation mechanism of diagonal wear (see chapter 2) which is one of the feature of the polygonal wear, by using the analytical model and from the analytical results treated in this report. At this stage, it is rational to mention that the generation mechanisms of polygonal wear and diagonal wear in which the wear grows obliquely from the outside of the shoulder part in the axial direction of tire have no immediate connection with each other. This is the subject for a future study.

6. Conclusions

In order to make clear the generation mechanism of the polygonal wear which is one of the abnormal wears of automobile tire, the authors performed the modeling and the analysis, and confirmed a very good agreement between the experimental and the theoretical results. The results obtained are summarized as follows:

(1) The generation mechanism of the pattern formation phenomenon caused by the first natural vibration mode of tire itself in the vertical direction was made clear by modeling a system with time lag in which the wear quantity of tire generated in the rolling contact surface is fed back to the contact surface after one rotation of tire as a forced displacement for the vibration in the vertical direction.

(2) Almost regular polygonal pattern is formed on the tire tread in the circumferential direction when the polygonal wear is generated. The generation regions are in some limited ones satisfying the relation of (natural frequency of tire) $\geq$ (polygonal number of tire) $\times$ (rotational frequency of tire). Especially, the polygonal wear phenomena are apt to be generated in some limited regions satisfying the relation of (natural frequency of tire) $\approx$ (polygonal number of tire) $\times$ (rotational frequency of tire).

(3) The difference in modeling of wear quantity of tire and wear resistance gives almost no effect upon the width of generation regions of polygonal wear. However, it gives a significant influence upon the generation rate (the degree of instability) of the polygonal wear. On the other hand, the damping takes directly part in the width of generation regions of polygonal wear.

(4) As the countermeasures of polygonal wear of tire, there are avoidance of traveling for a long time and at a constant speed, decrease of toe-in and camber angle, and improvement of the vibration characteristics of tire itself of the first order in the vertical direction.

Appendix

The polygonal wear of rear tires of a FF vehicle or of front tires and idle wheel tires of a FR vehicle, that is, of the follower tires is analyzed for the case that the actual vehicle is traveling on the road. Here, we obtain the equations of motion of the coupled vibration in the vertical direction between tire tread, unsprung mass and sprung mass. In Fig. 9, the analytical model is shown. The mass of the tire tread part is m_1, unsprung mass is m_2, sprung mass is m_3, contact stiffness and viscous damping coefficients due to air pressure between tire and road surface are k_1 and c_1, respectively, stiffness and damping coefficients of side wall part of tire between unsprung mass and tire tread are k_2 and c_2, respectively, and stiffness and damping

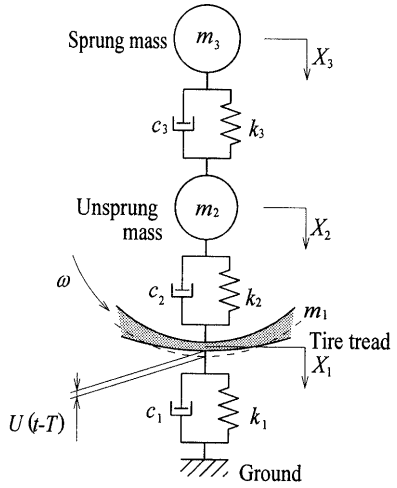

Fig. 9 Analytical model of a tire-mass system

coefficients of suspension between sprung and unsprung masses are k_3 and c_3, respectively. Let the displacements of tire tread, unsprung mass and sprung mass from the corresponding static equilibrium points in the gravity field be $X_1(t)$, $X_2(t)$ and $X_3(t)$, respectively. And let tire total wear quantity be $U(t)$. Then, the equation of motion is given as

$$\left.\begin{aligned} &m_1\ddot{X}_1(t)+c_2\{\dot{X}_1(t)-\dot{X}_2(t)\}+k_2\{X_1(t)-X_2(t)\}\\ &\quad+c_1\{\dot{X}_1(t)-\dot{U}(t-T)\}\\ &\quad+k_1\{X_1(t)-U(t-T)\}=0\\ &m_2\ddot{X}_2(t)+c_3\{\dot{X}_2(t)-\dot{X}_3(t)\}+k_3\{X_2(t)-X_3(t)\}\\ &\quad+c_2\{\dot{X}_2(t)-\dot{X}_1(t)\}+k_2\{X_2(t)-X_1(t)\}=0\\ &m_3\ddot{X}_3(t)+c_3\{\dot{X}_3(t)-\dot{X}_2(t)\}\\ &\quad+k_3\{X_3(t)-X_2(t)\}=0 \end{aligned}\right\} \tag{16}$$

Assuming that the instantaneous wear quantity is proportional to n-th power of the absolute value of lateral force, the total wear quantity is given as

$$\begin{aligned} U(t)=U(t-T)+\nu\beta^n[&P_0+c_1\{\dot{X}_1(t)-\dot{U}(t-T)\}\\ &+k_1\{X_1(t)-U(t-T)\}]^n \end{aligned} \tag{17}$$

where P_0 is a constant load due to sprung, unsprung masses and tire tread mass. Let the steady-state wear solutions of Eqs. (16) and (17) be $X_{10}(t)$, $X_{20}(t)$, $X_{30}(t)$ and $U_0(t)$, and let the corresponding small variations from the steady-state wear solutions be $x_1(t)$, $x_2(t)$, $x_3(t)$ and $u(t)$, respectively. Then, the linear equations with respect to the variations are given as

$$\left.\begin{aligned} &m_1\ddot{x}_1+c_2(\dot{x}_1-\dot{x}_2)+k_2(x_1-x_2)+c_1\{\dot{x}_1(t)\\ &\quad-\dot{u}(t-T)\}+k_1\{x_1(t)-u(t-T)\}=0\\ &m_2\ddot{x}_2+c_3(\dot{x}_2-\dot{x}_3)+k_3(x_2-x_3)\\ &\quad+c_2(\dot{x}_2-\dot{x}_1)+k_2(x_2-x_1)=0\\ &m_3\ddot{x}_3+c_3(\dot{x}_3-\dot{x}_2)+k_3(x_3-x_2)=0 \end{aligned}\right\} \tag{18}$$

$$\begin{aligned} u(t)=u(t-T)+\nu\beta^nP_0^{n-1}n[&c_1\{\dot{x}_1(t)-\dot{u}(t-T)\}\\ &+k_1\{x_1(t)-u(t-T)\}] \end{aligned} \tag{19}$$

Applying the variable transformation of Eq. (15) to Eqs. (18) and (19), and Laplace transformation with all the initial values equating to be zero yields

$$\boldsymbol{AX}=\boldsymbol{0} \tag{20}$$

where $\boldsymbol{X}={}^t[\tilde{X}_1(s), \tilde{X}_2(s), \tilde{X}_3(s), \tilde{U}(s)]$, and $\tilde{X}_1(s)$, $\tilde{X}_2(s)$, $\tilde{X}_3(s)$ and $\tilde{U}(s)$ are image functions after Laplace transformation of $x_1(t)$, $x_2(t)$, $x_3(t)$ and $u(t)$, respectively. The elements of matrix $\boldsymbol{A}=[a_{ij}]$ are expressed as

$$\begin{aligned} &a_{11}=m_1\omega^2s^2+(c_1+c_2)\omega s+k_1+k_2\\ &a_{12}=a_{21}=-(c_2\omega s+k_2),\quad a_{13}=a_{31}=0\\ &a_{14}=-(c_1\omega s+k_1)e^{-2\pi s}\\ &a_{41}=-\nu\beta^nP_0^{n-1}n(c_1\omega s+k_1)\\ &a_{22}=m_2\omega^2s^2+(c_2+c_3)\omega s+k_2+k_3\\ &a_{23}=a_{32}=-(c_3\omega s+k_3),\quad a_{24}=a_{42}=0\\ &a_{33}=m_3\omega^2s^2+c_3\omega s+k_3,\quad a_{34}=a_{43}=0\\ &a_{44}=1-\{1-\nu\beta^nP_0^{n-1}n(c_1\omega s+k_1)\}e^{-2\pi s} \end{aligned}$$

From Eq. (20), the characteristic equation becomes as

$$\det \boldsymbol{A}=0 \tag{21}$$

In numerical computation, the parameter values as shown in Tables 2 and 4 are used. In order to investigate the generation of the polygonal wear phenomenon, the damping coefficients indicated in Table 4 were set to the values a little smaller than the actual ones.

References

(1) Sueoka, A., Pattern Formations in Contact Rotating Systems, Frontier Technology of Rotor Dynamics, Preprint of JSME Lecture, (in Japanese), No. 930-23 (1993), p. 9.

(2) Edited by Japan Automobile Tire Manufacturer's Association Inc., On the abnormal wears of passenger car tire, (in Japanese), (1990), p. 2, JATMA.

(3) Sakai, H., Tire Engineering, (in Japanese), (1987), p. 294, Guranpuri Publishing.

(4) Fluegge, J. H., Sparks, J. D. and Vekselman, I. W., Tire Treadwear Experiment Using Taguchi Method, SAE Paper, No. 880580, (1988), p. 1.

(5) Shepherd, W. K., Diagonal Wear Predicted by a Simple Wear Model, MARC Report MFG, 0320, (1985), p. 1.

(6) Edited by Nagamatsu, A. et al., Dynamics Handbook Motion. Vibration. Control, (in Japanese), (1993), p. 903, Asakurashoten.

(7) Sakai, T., Nakamura, H., Kobayakawa, S. and Ohasi, Y., A Study on the Tire Wear Life Test Method, Preprint of Japan Soc. Mech. Eng., (in Japanese), No. 95-10, IV (1995), p. 162.

(8) Sueoka, A., Ryu, T., Kondou, T., Tsuda, Y., Katayama, K., Takasaki, K., Yamaguchi, M. and Hirooka, H., Polygonal Deformation of Roll-Covering Rubber, JSME Int. J. Ser. C, Vol. 39, No. 1, (1996), p. 1.